Analysis of the FIRE II flight experiment by means of a collisional radiative model

By T. E. Magin, M. Panesi†, A. Bourdon‡ AND A. Bultel¶

1. Motivation and objectives

During a hypersonic entry into Earth's atmosphere, a massive amount of freestream kinetic energy is converted across a strong shock wave into translational energy of the gas. Depending on the shock intensity, different physico-chemical processes may take place, such as excitation of the internal energy modes, dissociation of the molecules, ionization of the atoms and molecules. These non-equilibrium phenomena are strongly coupled to each other. At high re-entry speeds, a significant portion of the heating experienced by the spacecraft can be due to radiation and is highly influenced by the shape of the internal energy distribution function. Concentration of the gas species and distribution of their internal energy level populations can be estimated by means of either multi-temperature models (Gnoffo *et al*. 1989; Park 1990; Candler & MacCormack 1991) or collisional radiative models (Laux 2002; Capitelli *et al*. 2002; Bourdon & Bultel 2008*a*).

In the case of multi-temperature models, the flow physico-chemical properties are obtained through the shock layer by assuming that, for all the species, the population of each internal energy mode (rotational, vibrational and electronic mode) follows a Boltzmann distribution at a specific temperature (T_r rotational, T_v vibrational and T_e electronic temperature, respectively). In order to calculate these temperatures and the energy exchanged between all the energy modes (i.e. translational, rotational, vibrational and electronic), conservation equations for the internal energy modes in thermal non-equilibrium are added to the classical set of conservation equations for mass, momentum and total energy. The macroscopic rate coefficients for the chemical mechanism are assumed to depend on an empirical temperature that is a function of the different temperatures in the flow. It is important to mention that multi-temperature models are easy to implement in multi-dimensional flow codes and have been used extensively in the literature so far. Park (2006) has shown that the internal energy level populations may depart from Boltzmann distributions in expanding and compressing air flows. Therefore, the use of multi-temperature models, even if very efficient from a computational point of view, can only be justified when the departure from the Boltzmann population is small, i.e., for low velocity and high pressure re-entry conditions.

Collisional Radiative (CR) models take into account all relevant collisional and radiative mechanisms between the internal energy levels of the different species present in the flow. They constitute a valid alternative to the multi-temperature models since they exhibit a larger spectrum of applicability. By increasing order of complexity and computational time requirement, three kinds of CR models can be distinguished for air: *electronic* (Teulet *et al*. 2001; Bultel *et al*. 2006), *vibrational* (Chauveau *et al*. 2003; Park 2006) and *rovibrational* state-to-state models. In electronic state-to-state models,

† Aeronautics and Aerospace Department, von Karman Institute for Fluid Dynamics, Belgium
‡ Laboratoire EM2C – UPR 288 CNRS, Ecole Centrale Paris, France
¶ CORIA, CNRS UMR 6614 – Université de Rouen, France

transitions between the electronic states are considered and the rovibrational levels of the molecules are populated according to Boltzmann distributions at temperatures T_v and T_r. In vibrational state-to-state models, transitions between the vibrational states of the molecules are also considered and only a rotational temperature is defined. For both types of models, intensive computational time requirements do not allow for efficient implementation in multi-dimensional codes, most calculations are thus performed by means of 0-D and 1-D flow solvers. Finally, in rovibrational state-to-state models, no internal temperature is required. It is interesting to note that rovibrational models have not been proposed so far, due to the computational time limitations and lack of knowledge of the reaction rates.

When using CR models, we distinguish several ways to deal with time integration and coupling with flow solvers. The most widely used approach for time integration is the Quasi-Steady-State (QSS) approximation (Park 1990). This method is based on the simplifying assumption that the characteristic time of processes involving excited states is extremely fast compared to the one of the flow; therefore, concentrations of the species on excited states adjust almost instantaneously to the flow changes. The QSS assumption can be used either for all excited levels or only for a limited number of them (e.g., high-lying electronic levels). Various QSS CR models have been used in 0-D. For example, the electronic state-to-state models given in Teulet *et al*. (2001) and the vibrational state-to-state model given in Chauveau *et al*. (2003) have been developed to study non-equilibrium effects in recombining plasmas at atmospheric pressure characterized by a free electron temperature larger than the heavy-particle temperature. QSS CR models can be loosely coupled to flow codes (Park 1990); the profiles of the thermodynamic variables (pressure, temperatures and species mass fractions) are derived based on a flow calculation, then the populations of excited states are obtained at each desired location in the flow by means of a QSS CR model. Johnston (2006) has used this approach to study the influence of the non-equilibrium distribution of the electronic energy levels of atoms and molecules of air after a strong shock and has shown that non-equilibrium populations strongly affect the radiative heat fluxes.

The second approach for time integration is the so-called time-dependent CR model, in which balance equations are solved simultaneously for all species on ground and excited states without any constraint on the relaxation times of the excited levels. Recently, a time-dependent electronic state-to-state CR model for air has been developed and used in 0-D by Bultel *et al*. (2006). Different typical re-entry flow conditions have been studied and significant differences have been observed between the species concentrations calculated with their CR model and some widely used multi-temperature kinetic mechanisms. Time-dependent CR models can be either loosely or directly coupled to flow codes. The loosely coupled, or Lagrangian approach, is particularly well-adapted when the concentrations of excited states are much lower than those of the ground state. In this method, the profiles of the thermodynamic variables are also derived based on a flow computation. Then, in a second step, the excited species mass fractions are obtained by following accurately in time a cell of fluid. For example, this method has been used for entries into the atmosphere of Titan (Magin *et al*. 2006); for low-pressure conditions, significant deviations of the excited electronic state populations of nitrogen molecules from QSS predictions have been observed in the near-shock region. In the directly coupled approach, state-to-state equations are solved simultaneously with classical conservation equations of the flow, this approach is the most general one. Capitelli *et al*. (2002) have studied vibrational non-equilibrium in supersonic air nozzle flows. Park (2006) has shown

that the populations of upper vibrational levels deviate from a Boltzmann equilibrium and are strongly affected by the air chemistry, in particular, by the Zel'dovich reaction between molecular nitrogen and atomic oxygen.

In this work, we propose to study FIRE II (Cauchon 1967), a flight experiment carried out in 1960s to estimate the heating experienced by a capsule at high re-entry speeds ($\geq$ 10 km/s). The data, collected by measuring directly the incident radiation using on-board radiometers, can be used for the validation of flow solver and physical models. In the analysis that follows, we focus our attention on three trajectory points: 1634 s, 1636 s and 1643 s (elapsed time from the launch). The first two points chosen belong to the earlier part of the trajectory where the flow exhibits strong non-equilibrium effects, whereas for the last point under consideration, the gas is close to equilibrium conditions. The investigation is carried out by means of a hybrid model that combines the use of an electronic state-to-state CR model for the electronic levels of the nitrogen and oxygen atoms and describes the thermal non-equilibrium effects of the energy modes of the other species by means of a multi-temperature model. This choice is justified for the high temperatures reached at high-speeds ($\geq$ 10 km/s), since the contribution to the radiative component of the heat flux is dominated by atomic lines and continuum radiation (Johnston 2006; Bose *et al*. 2006), the molecules being almost completely dissociated in this temperature range. The rates of the electronic-specific reactions are based on the data of the electronic state-to-state CR model recently developed by Bultel *et al*. (2006). Our time-dependent CR model is directly coupled with a 1-D flow solver to simulate shock-tube experiments, allowing for a thorough analysis of the validity of the QSS assumption. Conservation equations of mass, momentum, global energy, vibrational energy and free-electron energy are solved simultaneously. The large number of elementary processes considered in the model allows for a better understanding of the kinetic mechanisms for air plasmas.

2. Physico-chemical model

2.1. *Collisional radiative model*

In this study, we consider a mixture of nitrogen and oxygen and their products: N_2, O_2, NO, $N(1-46)$, $O(1-40)$, N_2^+, O_2^+, NO^+, N^+, O^+ and e^-, accounting for 46 electronic energy levels for atomic nitrogen and 40 levels for atomic oxygen, allowing for accurate calculation of (a) ionization of the N and O atoms by electron impact; (b) the net population of the metastable states resulting from electron-induced processes. Coupling of the atom electronic energy levels through the different elementary processes allows for explicit determination of their excitation and the radiative signature of the plasma without using any *a priori* assumption on their populations. The vibrational energy level populations of the N_2, O_2, and NO molecules are assumed to follow Boltzmann distributions at the vibrational temperatures $T_{v\mathrm{N}_2}$, $T_{v\mathrm{O}_2}$ and $T_{v\mathrm{NO}}$, respectively; the vibrational populations of the other molecules are associated with the vibration of the N_2 molecule. The rotational energy level populations are assumed to follow Boltzmann distributions at the translational temperature T of the gas. The CR model yields the electronic state populations of the N and O atoms. Thus, their electronic temperature does not need to be specified. The electronic energy populations of the other species are assumed to follow Boltzmann distributions at the translational temperature T_e of the free electrons. In this work, we assume one common temperature $T_{v\mathrm{N}_2} = T_e$ for the vibration of N_2 and for the translation of the free electrons and electronic excitation of the species following a Boltzmann distribution. The rates of the electronic-specific reactions are based on the

data of the electronic state-to-state CR model recently developed by Bultel *et al.* (2006). A complementary set of reaction rates is taken from Park *et al.* (2001). For excitation and ionization of the higher states of N and O, we have used the cross-sections proposed by Drawin (1969) and expressed the rate coefficients under an analytical form derived from integration of these cross-sections over a Boltzmann distribution at the electron T_e. At speeds higher than 10 km/s, the radiative signature is based on spontaneous emission of the N and O atoms by grouping elementary levels having similar characteristics. The equivalent spontaneous emission probability of each level has been computed based on the NIST (National Institute of Standards and Technology) database, in total, 45 spontaneous emission lines for N and 24 lines for O.

2.2. *Shock-tube flow solver*

We have developed a 1-D flow solver for simulation of air plasmas obtained in shock-tube facilities, based on the model proposed by Magin *et al.* (2006), modified to simulate re-entries at speeds $\geq$ 10 km/s. A radiative source term Q_{Rad} has been added in the equation that expresses conservation of the total energy, since radiative transitions tend to deplete the flow energy for an optically thin medium. The contribution of the free electron energy has been considered, since the flow is significantly ionized.

2.2.1. *Conservation equations*

Post-shock conditions are derived from jump relations assuming frozen gas composition and vibrational-electronic energy modes, the rotational mode being in equilibrium with the translational mode. Then, the downstream flowfield is found by solving conservation equations of mass, momentum, global energy, vibrational energy of the N_2 molecule coupled with the free electron energy and Boltzmann-type electronic energy, and finally, vibrational energy of the O_2 and NO molecules, respectively,

$$\frac{\partial}{\partial x}\left(\rho_i u\right) = M_i\,\dot{\omega}_i, \qquad i \in \mathcal{S} \tag{2.1}$$

$$\frac{\partial}{\partial x}\left(\rho u^2 + p\right) = 0 \tag{2.2}$$

$$\frac{\partial}{\partial x}\left[\rho u\left(h + \tfrac{1}{2}u^2\right)\right] = -Q^{Rad} \tag{2.3}$$

$$\begin{aligned}\frac{\partial}{\partial x}[\rho u(y_{\mathrm{N}_2} e^V_{\mathrm{N}_2} + y_e e_e + \sum_{i\in\mathcal{E}} y_i e^E_i)] = p_e\frac{\partial u}{\partial x} + M_e\,\dot{\omega}_e e^F_e + \sum_{i\in\mathcal{E}} M_i\dot{\omega}_i e^E_i - \Omega^{Ch} \\ +\Omega^{ET} + M_{\mathrm{N}_2}\,\dot{\omega}_{\mathrm{N}_2} e^V_{\mathrm{N}_2} + \Omega^{VT}_{\mathrm{N}_2} + \Omega^{VV}_{\mathrm{N}_2}\end{aligned} \tag{2.4}$$

$$\frac{\partial}{\partial x}\left(\rho u y_m e^V_m\right) = M_m\,\dot{\omega}_m e^V_m + \Omega^{VT}_m + \Omega^{VV}_m,\ m \in \{\mathrm{O}_2, \mathrm{NO}\}. \tag{2.5}$$

Symbol $\mathcal{S}$ stands for the set of indices of the mixture species and $\mathcal{E}$, the set of indices of the N^+, O^+, N_2, O_2, NO, N_2^+, O_2^+ and NO^+ species, whose electronic energy populations are assumed to follow Boltzmann distributions. Symbols $\mathcal{N}$ and $\mathcal{O}$ stand for the set of indices of the electronic energy levels of the N and O atoms. Thus, the set of indices of the heavy particles is given by $\mathcal{H} = \mathcal{N} \cup \mathcal{O} \cup \mathcal{E}$ and the set of the mixture species by $\mathcal{S} = \mathcal{H} \cup \{\mathrm{e}\}$. The mass density of species i reads ρ_i, and its molar mass, M_i. The mixture mass density is given by the expression $\rho = \sum_{j\in\mathcal{S}} \rho_j$, the mixture energy, $e = \sum_{j\in\mathcal{S}} y_j e_j$, with the mass fraction $y_i = \rho_i/\rho$, the mixture enthalpy $h = e + p/\rho$, the pressure $p = \rho RT \sum_{j\in\mathcal{H}} (y_j/M_j) + \rho R T_e y_e/M_e$, the flow velocity u. The species energy e_i, $i \in \mathcal{S}$, comprises the translational and formation contributions $[e_e = e^T_e(T_e) + e^F_e]$ for

electrons; the translational, electronic, and formation contributions $[e_i = e_i^T(T)+e_i^E+e_i^F]$ for the electronic energy states N(i), $i \in \mathcal{N}$, and O(i), $i \in \mathcal{O}$; the translational, electronic, and formation contributions $[e_i = e_i^T(T) + e_i^E(T_e) + e_i^F]$ for the N^+ and O^+ ions; and the translational, rotational, vibrational, electronic, and formation contributions $[e_i = e_i^T(T) + e_i^R(T) + e_i^V(T_{vi}) + e_i^E(T_e) + e_i^F]$ for all the molecules, where T_{vi} is the vibrational temperature of the i molecule. Energy of molecules is computed assuming the rigid rotor and harmonic oscillator approximations based on electronic specific data.

2.2.2. *Energy relaxation terms*

Radiative losses are modeled by means of the Q^{Rad} term, radiant power emitted per unit volume. At high-speeds, it is important to account for the energy lost by the free electrons during ionization and excitation of the atoms and molecules. Otherwise, electron impact ionization reactions, and in general all the reactions involving free electrons, produce a large amount of free electrons without depleting their kinetic energy, thus enhancing their production. This phenomenon may lead to an avalanche ionization with consequent related numerical problems, especially for high-speed conditions. The expression for the related source term for electron-impact ionization and excitation reactions reads

$$\Omega^{Ch} = \sum_{r \in \mathcal{R}} \dot{\omega}_{e,r} \Delta\mathcal{H}^r, \tag{2.6}$$

where $\Delta\mathcal{H}^r$ is the reaction enthalpy of the r reaction, and $\dot{\omega}_{e,r}$, the electron chemical production term of the r reaction. Symbol $\mathcal{R}$ denotes the set of indices of the electron-impact ionization and excitation reactions. The rate of vibrational-translational energy transfer Ω_m^{VT} follows a Landau-Teller formula with an average relaxation time based on Millikan-White's formula including Park's correction. For the vibrational-vibrational energy exchange Ω_m^{VV}, the formula proposed by Candler & MacCormack (1991) with Knab's correction has been chosen. The energy lost by electrons through elastic collisions with heavy particles is Ω^{ET}. To model the exchange between the vibrational energy and the free-electron energy, we only consider molecular nitrogen, since this molecule is more efficient than O_2 and NO for this kind of process. This rate is assumed to follow a Landau-Teller formula.

3. Results

In this section, we apply the collisional radiative model to a simulation of the FIRE II flight experiment, for different physico-chemical conditions from electronic energy level populations in strong non-equilibrium to populations following Boltzmann distributions. The set of operating conditions corresponding to these three trajectory points is found in Table 1. Freestream characteristic quantities are denoted by the subscript $_1$, post-shock characteristic quantities by the subscript $_2$. The mole fractions of nitrogen and oxygen are assumed to be constant through the shock ($x_{N_2} = 0.79$ and $x_{O_2} = 0.21$). We recall that, after the shock, the rotational temperature is equal to the post-shock gas temperature T_2, whereas the vibrational and electron temperatures are still equal to the freestream gas temperature T_1. Starting from the earliest trajectory points (1634 s and 1636 s), we move to a description of a point approaching peak heating (1643 s). The validity of the QSS assumption, often used to compute the excited electronic states, is investigated for the 1634 s case by comparing the electronic energy level populations of atomic nitrogen

Time [s]	p_1 [Pa]	T_1 [K]	u_1 [m/s]	p_2 [Pa]	T_2 [K]	u_2 [m/s]
1634	2.0	195	11,360	3827	62,377	1899
1636	5.25	210	10,480	9229	61,884	1891
1643	21.3	276	10,480	24,506	53,191	1756

TABLE 1. Shock-tube flow characteristic quantities.

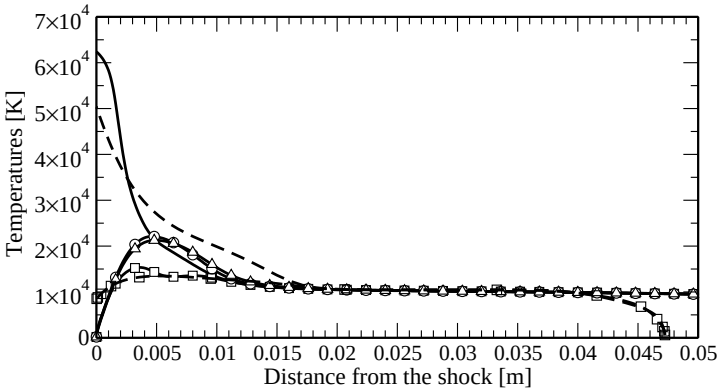

FIGURE 1. 1634 s case, temperature profiles obtained by means of the CR model: $T = T_r$ (unbroken line), $T_{v\mathrm{N}_2} = T_e$ (line with squares), $T_{v\mathrm{O}_2}$ (line with triangles), $T_{v\mathrm{NO}}$ (line with circles); Johnston's results: $T = T_r$ (dashed line), $T_v = T_e$ (dashed line with squares).

obtained with the QSS assumption to the populations obtained by means of the full CR model.

3.1. *Analysis of the Fire II 1634 s case*

3.1.1. *Temperatures, composition and electronic energy populations*

In Fig. 1, we compare our four-temperature profiles ($T = T_r$, $T_{v\mathrm{N}_2} = T_e$, $T_{v\mathrm{O}_2}$ $T_{v\mathrm{NO}}$) with the two-temperature profiles ($T = T_r$, $T_v = T_e$) obtained by Johnston (2006). While the vibrational free-electron temperature results agree quite well, discrepancies are found in the relaxation of the ro-translational temperature. In Fig. 2, we examine the evolution of the concentrations for the different species and the electronic energy level population for atomic nitrogen. We recall that only molecular nitrogen and oxygen are present after the shock. These molecules first dissociate, in particular, molecular oxygen tends to completely disappear in favor of atomic oxygen right after the shock, while the full dissociation of molecular nitrogen is delayed. Ionization occurs simultaneously and produces free electrons, nitrogen atom ionization being more efficient than ionization of the other species. The upper electronic states are more reactive than the ground state and lower (metastable) states. Immediately after the shock, the populations of the excited levels are driven by the free electron populations that are in non-equilibrium. Moreover, the atom populations are mainly in the ground electronic state at the beginning of the relaxation, consistent with the kinetic mechanism assuming that dissociation of molecular nitrogen and oxygen generates atoms in the ground state: $\mathrm{N}_2 + \mathrm{M} \rightleftharpoons \mathrm{N}(1) + \mathrm{N}(1) + \mathrm{M}$ and $\mathrm{O}_2 + \mathrm{M} \rightleftharpoons \mathrm{O}(1) + \mathrm{O}(1) + \mathrm{M}$. The same assumption holds for all the other reactions (in particular for the Zel'dowich reaction responsible for the atomic nitrogen formation). This assumption is justified since electronic excitation mainly occurs via electron impacts;

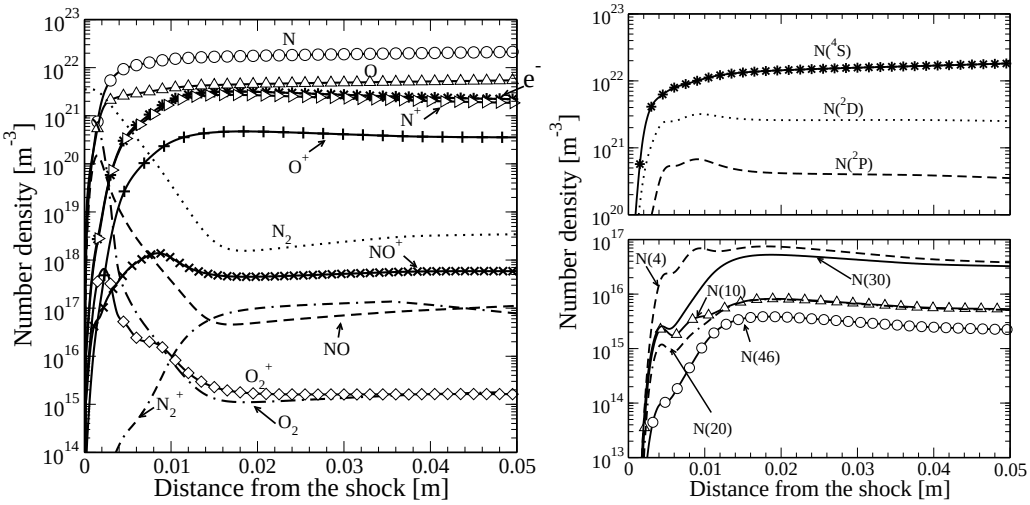

FIGURE 2. 1634 s case, number density profiles obtained by means of the CR model. Left: mixture species N_2, O_2, NO, N, O, N_2^+, O_2^+, NO^+, N^+, O^+, e^-; right: electronic energy levels N(1), N(2), N(3), N(4), N(10), N(20), N(30), N(40).

the number density of electrons is still low in the post-shock region. After an incubation distance where the number density of electrons significantly increases, the electronic states of atoms thermalize. The electron-impact excitation processes, $\mathrm{O(i)} + \mathrm{e^-} \rightleftharpoons \mathrm{O(j)} + \mathrm{e^-}$ and $\mathrm{N(i)} + \mathrm{e^-} \rightleftharpoons \mathrm{N(j)} + \mathrm{e^-}$, are fast and the populations of excited electronic states rapidly increase. The upper states are then depleted, in particular by ionization and spontaneous emission, which explains the maximum found in the population profiles.

The number density of the electronic states of atomic nitrogen is compared in Fig. 3 at two locations after the shock with the Boltzmann and Saha distributions computed based on the electron temperature T_e by keeping the atomic nitrogen concentration constant. In logarithmic scale, these distributions appear as two parallel straight lines of slope proportional to $-1/T_e$. At 0.7 cm from the shock, the CR model predicts that the ground and metastable states follow the Boltzmann distribution, whereas the number density of the highly excited states is much lower and tend to the Saha distribution. This phenomenon is typical of non-equilibrium conditions encountered during high-speed re-entries. Excellent agreement is found with the results presented in Johnston (2006). Moving 2.5 cm from the shock front, the flow tends toward equilibrium, and the Saha distribution tends to the Boltzmann distribution. Our model predicts that the high-lying excited states are still being depleted by radiative exchange with lower states. Our results show a higher degree of non-equilibrium than in Johnston (2006), closer to the Boltzmann distribution.

3.1.2. *Standard QSS model*

Quasi-steady-state models (Park 1990) constitute a valid alternative to the time-dependent CR model presented in this paper when the characteristic time of the excited state processes is very short with respect to the characteristic time of the flow. As a consequence, the set of mass conservation equations for the electronically excited states given in Eq. (2.1) can be expressed as a set of non-linear algebraic equations to be solved separately from the other conservation equations. It is important to emphasize that this operation does not reduce the computational cost if the electronic energy populations

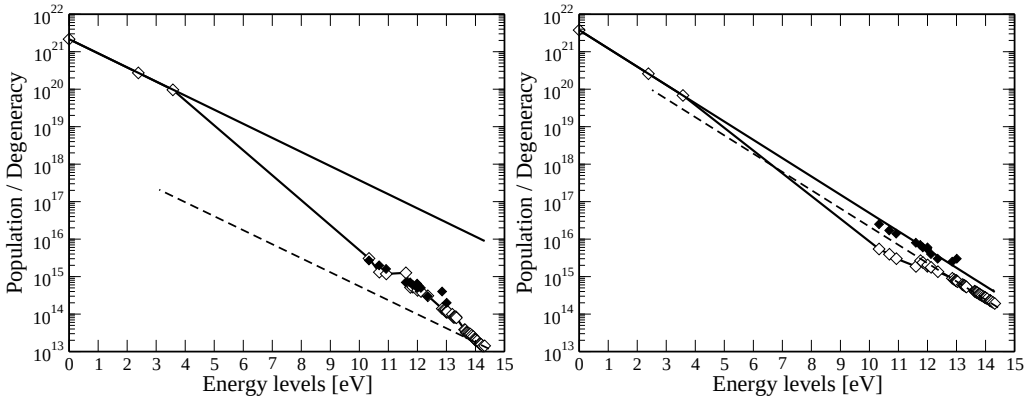

FIGURE 3. 1634 s case, electronic energy level populations for atomic nitrogen [m^{-3}]: CR model (line with diamonds), Boltzmann distribution (unbroken line), Saha distribution (dashed line), and Johnston's results (black diamonds). Left: 0.7 cm from the shock front, right: 2.5 cm.

are computed everywhere in the flow. The QSS assumption is only desirable when the populations of excited states are probed at some locations of interest, for instance, along the stagnation line in multi-dimensional flow simulations, and therefore allowing for a drastic reduction of the computational cost versus the time-dependent CR model.

It is well-known that the regime of validity of the QSS assumption is strongly influenced by a sudden change in the plasma conditions, such as after a strong shock where the electron density is very scarce. Since the collisional processes are responsible for the equilibration of the internal energy states, in particular the processes involving electrons as collision partners, a lack of electrons contributes to the failure of the QSS assumption.

In the following analysis, we examine the first trajectory point at a location of 0.7 cm from the shock front. We compute the electronic energy populations of nitrogen atoms based on three models:

(a) Full CR: the time-dependent CR model described in Sec. 2,

(b) QSS Abba: QSS model with the same data for the atomic and radiative elementary processes as in the full CR model,

(c) QSS Park: QSS model with the energy levels and data for the atomic and radiative elementary processes of Park (1990).

The main differences between the various models are the coupling method and the sets of data for the reaction rates. For both QSS models, the flow calculations have been performed by clipping the reaction rates of Park *et al.* (2001) in order to avoid using them out of their validity range; the translational temperature driving the rate constants has been limited to the value of 30 000 K. Moreover, the free-electron energy loss term for electron-impact ionization given in Eq. (2.4) is computed based on the expression suggested in Johnston (2006), $\Omega^{Ch} = -\omega_{N^+} I^{N^+} - \omega_{O^+} I^{O^+}$, where $I^{N^+} = 4.05 \times 10^8$ J/(kg mol) and $I^{O^+} = 4.30 \times 10^8$ J/(kg mol), respectively. In the full CR model, we recall that this term is directly computed based on Eq. (2.6) from the expressions for the reaction rates intrinsic to the model, without any *a priori* hypothesis.

Figure 4 shows a comparison between the results obtained by means of the three models, the Boltzmann distribution and Johnston's results. The full CR model and the QSS Abba model yield electronic energy level populations in rather good agreement with Johnston's results. The QSS Abba model slightly underpredicts the population of the lower electronic levels. The QSS assumption is a fair approximation at this location.

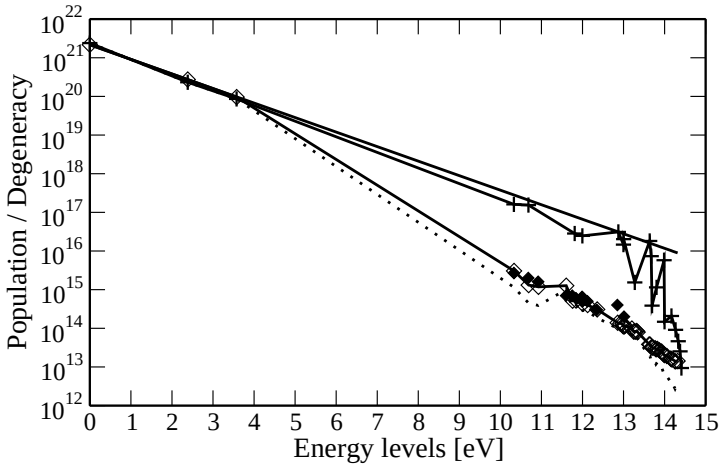

FIGURE 4. 1634 s case, 0.7 cm from the shock front, electronic energy level populations for atomic nitrogen [m^{-3}]: full CR model (line with diamonds), QSS Abba model (dotted line), QSS Park model (line with crosses), Boltzmann distribution (unbroken line) and Johnston's results (black diamonds).

The differences between the QSS Abba results and the QSS results of Johnston are not well-understood and might be explained by the different data for the electron-impact excitation rates of atoms or for the radiative processes. The differences with respect to the QSS Park model for atomic and radiative processes are significant: up two orders of magnitude for the upper levels above the metastable states. In conclusion, the standard QSS approach is valid, *at this location*, provided that a correct set of reaction rates is chosen for the model. This choice should be based on a comparison of the computed results with experimental data.

3.1.3. *Toward a simplified CR model*

In this section, we further investigate the validity of the QSS assumption, based on the same set of reaction rates, at several locations in the flow. This is a preliminary step to derive a simplified CR model for re-entries at speeds higher than 10 km/s, typical of returns from the Moon. For this purpose, we compute the electronic energy populations of atomic nitrogen for the first trajectory point (1634 s case) by means of the full CR model. From the calculation, we extract the profiles of the flow characteristic quantities (pressure, temperatures and composition). Then, the QSS populations of excited electronic states are computed at a given location; this approach is the so-called "simplified CR model." The flow is investigated at two locations: 0.3 cm and 1 cm from the shock. The electronic energy level populations for atomic nitrogen are shown in Fig. 5. At 0.3 cm, the populations obtained by means of the simplified CR model are higher than the populations obtained by means of the full CR model; the QSS assumption is not valid in the near-shock region. This difference of populations is much more pronounced for the metastable states that follow a Boltzmann distribution when the QSS assumption is used. After 1 cm, no difference is noticed between the results obtained by means of the two models. An explanation is found by examining the characteristic time for the atomic excitation and ionization processes. For instance, we find that this characteristic time for the first metastable state is of the same order of magnitude as the characteristic time of the flow 5×10^{-6} s computed at 1 cm from the shock. Based on this analysis, we recom-

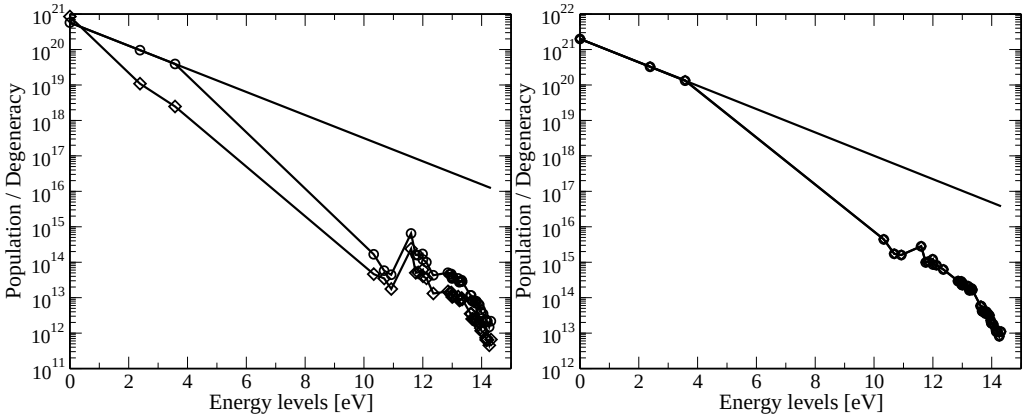

FIGURE 5. 1634 s case, electronic energy level populations for atomic nitrogen [m^{-3}]: simplified CR model (line with circles), full CR model (line with diamonds), Boltzmann distribution (unbroken line). Left: 0.3 cm from the shock; right: 1 cm from the shock.

mend keeping the atomic metastable states as separate species for this trajectory point and computing the upper electronic states by means of a QSS model, in order to reduce the computational cost in multi-dimensional flow simulations. The CR model could be used as a tool to derive effective reaction rates for the simplified mechanism associated with this mixture of species and also the expressions for the free-electron energy loss term for electron-impact ionization and ionization reactions.

3.2. *Analysis of the Fire II 1636 and 1643 s cases*

In Fig. 6, the electronic energy level populations for atomic nitrogen are shown at 0.5 cm from the shock front for two trajectory points. For the 1636 s case, the low electronic energy levels tend to follow a Boltzmann distribution at the electron temperature, whereas, close to the ionization limit, the excited electronic states approach a Saha distribution at the electron temperature. Since the channels between the low- and high-lying electronic states exhibit finite ionization rates, a lack of free electrons may result in depleted populations for the highly excited states. The distribution is no longer of Boltzmann type and the electronic temperature is no longer defined. The departures from the Boltzmann distribution, which are of the same order of magnitude for atomic nitrogen and atomic oxygen, tend to reduce the radiative contribution to the overall heat flux in the earlier parts of the trajectory. For this reason, attempts to estimate the radiative flux assuming a Boltzmann distribution among electronic levels might lead to an over-estimation of this heat flux. For the 1643 s case, the thermal non-equilibrium effects are located in a very narrow region near the shock. The electronic energy level populations of atomic nitrogen follow Boltzmann distributions at 0.5 cm from the shock. These results are explained by the values of the post-shock pressure p_2 given in Table 1, much higher than for the first two trajectory points. At high pressures, the plasma is dominated by collisional processes.

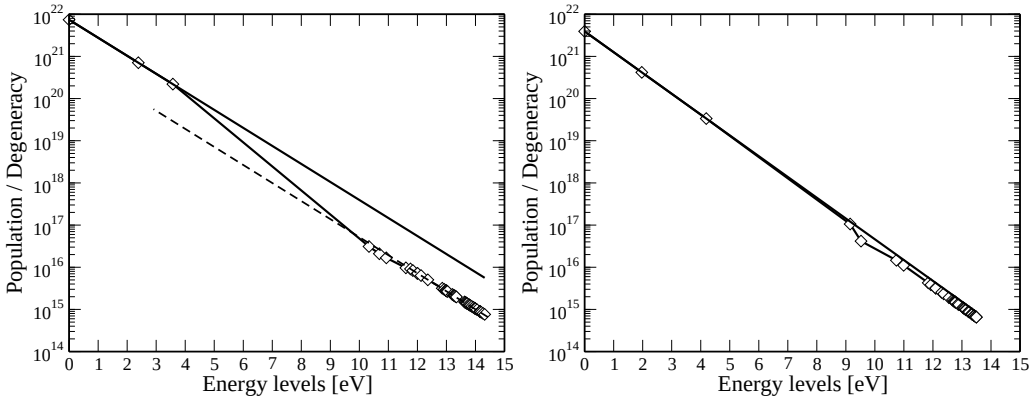

FIGURE 6. Electronic energy level populations for atomic nitrogen 0.5 cm from the shock front [m^{-3}]. CR model (line with diamonds), Boltzmann distribution (unbroken line), Saha distribution (dashed line). Left: 1636 s case, right: 1643 s case.

4. Conclusions

In this work, we have studied the departure of the atomic electronic energy populations from Boltzmann distributions for 1-D air flow simulations for three trajectory points of the FIRE II flight experiment. The results have been obtained by means of a multi-temperature fluid model fully coupled with an electronic-specific collisional radiative model. We have found a good agreement with literature (Johnston 2006) for the flowfield quantities and electronic energy populations. For the first two trajectory points (1634 s and 1636 s), the electronic energy level populations of the N and O atoms depart from Boltzmann distributions since the high-lying bound electronic states are depleted. The analysis of the last trajectory point (1643 s) reveals instead a Boltzmann distribution among the electronic energy levels.

For the first flight condition (1634 s), we have also assessed a standard QSS model widely used in the aerospace community. The populations of high-lying excited states of atoms obtained by using the standard rates of Park (1990) for electron-impact excitation and ionization reactions are up to two orders of magnitude higher than the populations obtained by using the rates of Bultel *et al.* (2006), consistently with the results of Johnston (2006). The excited species of atoms satisfy the quasi-steady-state assumption, except for their two metastable states. It is important to mention that the full CR model is more general than the standard QSS model, since the parameters governing the free-electron energy losses by electron impact ionization are directly obtained from the expressions for the reaction rates intrinsic to the model, without any *a priori* hypothesis. We recommend that be derived global rate coefficients and free electron energy loss terms in the steady state based on our model, considering the metastable states as separate pseudo-species governed by their own chemical-kinetic mechanism.

5. Future work

We are currently adding the electronic energy levels of the molecules in the CR model (Panesi *et al.* 2008) and consider the vibrational energy levels of molecules as well, accounting for their vibrational non-equilibrium (Bourdon *et al.* 2008*b*). These phenomena, generally less important in flows subjected to compression, might become relevant in expanding flow situations affecting the vibrational populations of molecular species that,

as a consequence, can depart also from Boltzmann distributions. In a further work, we will use the detailed CR model as a baseline to create reduced kinetic mechanisms for air flow conditions typical of re-entry applications. The number of electronic levels of atoms and molecules considered in the model can be reduced by grouping similar energy levels. This will allow us to extend the use of the CR model for 2-D and 3-D computational fluid dynamic simulations.

Acknowledgement

The authors would like to acknowledge Dr. S. Macheret (Lockheed Martin Skunk Works) for useful suggestions on the free electron energy model and Dr. C. O. Johnston (NASA Langley Research Center) for providing the results used in the comparison.

REFERENCES

Bose, D., McCorkle, E., Thompson, C., Bogdanoff, D., Prabhu, D., Allen, G. A. & Grinstead, J. 2008 Analysis and model validation of shock layer radiation in air. *46th AIAA Aerospace Sciences Meeting and Exhibit.* January 7-10, Reno, Nevada. AIAA paper 2008–1246.

Bourdon, A., Bultel, A., Panesi, M. & Magin, T. E. 2008a Detailed and simplified kinetic mechanisms for high enthalpy air flows. *Course on hypersonic entry and cruise vehicles.* Chazot *et al.*, Rhode-Saint-Genèse, Belgium, VKI LS 2008-07.

Bourdon, A., Panesi, M., Brandis, A., Magin, T. E., Chaban, G., Huo, W., Jaffe, R. & Schwenke D. W. 2008b Simulation of flows in shock-tube facilities by means of a detailed chemical mechanism for nitrogen excitation and dissociation. *Proceedings of the Summer Program 2008*, Center for Turbulence Research, Stanford University, NASA Ames Research Center.

Bultel, A., Chéron, B. G., Bourdon, A., Motapon, O. & Schneider, I. 2006 Collisional-radiative model in air for Earth re-entry problems. *Physics of Plasmas* **13** (4), 11.

Candler, G. V. & MacCormack, R. W. 1991 Computation of weakly ionized hypersonic flows in thermochemical nonequilibrium. *Journal of Thermophysics and Heat Transfer* **5** (11), 266.

Capitelli, M., Colonna, G. & Armenise, I. 2002 State-to-state electron and vibrational kinetics in 1-D nozzle and boundary layer flows. *Physico-chemical models for high enthalpy and plasma flows.* Fletcher *et al.*, Rhode-Saint-Genèse, Belgium, VKI LS 2002–7.

Cauchon, D. L. 1967 Radiative heating results from FIRE II flight experiment at a re-entry velocity of 11.4 km/s. NASA Technical Memorandum X-1402.

Chauveau, S. M., Laux, C. O., Kelley, J. D. & Kruger, C. H. 2002 Vibrationally specific collisional-radiative model for nonequilibrium air plasmas. *33th AIAA Plasmadynamics and Lasers Conference.* May 20-23, Maui, Hawaii. AIAA paper 2002–2229.

Drawin, H. W. 1969 Influence of atom-atom collisions on the collisional-radiative ionization and recombination coefficients of hydrogen plasmas. *Zeitschrift für Physik* **225**, 483.

Gnoffo, P. A., Gupta, R. N. & Shinn, J. L. 1989 Conservation equations and

physical models for hypersonic air flows in thermal and chemical nonequilibrium. NASA Technical Paper 2867.

Johnston, C. O. 2006 *Nonequilibrium shock-layer radiative heating for Earth and Titan entry.* Ph.D. thesis, Virginia Polytechnic Institute and State University, Virginia.

Laux, C. O. 2002 Radiation and nonequilibrium collisional radiative models. *Physico-chemical models for high enthalpy and plasma flows.* Fletcher *et al.*, Rhode-Saint-Genèse, Belgium, VKI LS 2002–7.

Magin, T. E., Caillault, L., Bourdon, A. & Laux, C. O. 2006 Nonequilibrium radiative heat flux modeling for the Huygens entry probe. *Journal of Geophysical Research - Planets* **111**, E07S12.

Panesi, M., Magin, T., Bourdon, A., Bultel, A. & Chazot, O. 2008 Analysis of the Fire II Flight experiment by means of a collisional radiative model. *46th AIAA Aerospace Sciences Meeting and Exhibit.* January 7-10, Reno, Nevada. AIAA paper 2008–1205.

Park, C. 1990 *Nonequilibrium hypersonic aerothermodynamics.* New York: Wiley.

Park, C., Jaffe, R. & Partridge, H. 2001 Chemical-kinetic parameters of hyperbolic Earth entry. *Journal of Thermophysics and Heat Transfer* **15** (1), 76.

Park, C. 2006 Thermochemical relaxation in shock tunnels. *Journal of Thermophysics and Heat Transfer* **20** (4), 689.

Teulet, P., Sarrette, J.-P. & Gomes A.-M. 2001 Collisional-radiative modelling of one- and two- temperature air and air-sodium plasmas at atmospheric pressure with temperatures of 2000 - 12,000 K. *Journal of Quantitative Spectroscopy and Radiative Transfer* **70** (2), 159.